Adaptive Tuning of Frequency Thresholds Using Voltage Drop Data in Decentralized Load Shedding

Bakhtyar Hoseinzadeh, *Student Member, IEEE*, Filipe Miguel Faria da Silva, *Member, IEEE*, and Claus Leth Bak, *Senior Member, IEEE*

***Abstract*—Load shedding (LS) is the last firewall and the most expensive control action against power system blackout. In the conventional under frequency LS (UFLS) schemes, the load drop locations are already determined independently of the event location. Furthermore, the frequency thresholds of LS relays are prespecified and constant values which may not be a comprehensive solution for widespread range of possible events. This paper addresses the decentralized LS in which the instantaneous voltage deviation of load buses is used to determine the frequency thresholds of LS relays. The higher frequency thresholds are assigned to the loads with larger voltage decay which are often located in the vicinity of disturbance location. The proposed method simultaneously benefits from individual UFLS and under voltage LS (UVLS) features which operate in the power system without coordination. Numerical simulations in DigSilent PowerFactory software confirm the efficiency of proposed methodology in the stabilization of the power system after various severe contingencies.**

***Index Terms*—Adaptive frequency threshold, decentralized under voltage load shedding, protection relay.**

I. Introduction

POWER systems consist of numerous equipments with nonlinear dynamics and may not be properly protected by constant and prespecified settings of under frequency load shedding (UFLS) relays which are independent of the location and magnitude of the disturbance [1], [2]. Moreover, there is the risk of simultaneous operation of different relays distant from the event location due to having the same frequency threshold settings which may worsen the situation. To the best knowledge of authors, there is no comprehensive and widely used method to set the UFLS relay settings [3].

Dropping the loads distant from the disturbance place, may cause transmission line over loading, worse voltage profiles and power factor decline [1], [4]. Contrariwise, the load relief close to the event point is strongly recommended [5]–[7]. The buses nearby the failure place often experience larger voltage reduction. The voltage is an available variable to measure locally in all load bus relays. Thus, voltage drop information may be employed as a proper criterion of proximity to the failure point in power system analysis [7]–[10]. As a result, the loads may be classified to shed based on their voltage decay, which means the loads with higher voltage drop are discarded first. According to the proposed criterion, the LS process is initiated from the vicinity of the event location and radially propagates in the power system, so that not only the frequency collapse is prevented in time, but also the frequency returns back into the normal range [5], [11].

The work carried out in [6] advocates of exploiting the reactive power together with active power directly in the LS process. This technique deals with the coordination of voltage and frequency information in the centralized strategy of LS instead of independent methods. The technique proposed in [7] tries to determine the settings of frequency sensitive (FS) and frequency droop (FD) relays off line using frequency and rate of change of frequency (ROCOF) information under an abnormal condition.

Paper [9] concentrates on analyzing the overlooked factors that influence the frequency gradient and result in misleading information about the real active power deficit estimated using ROCOF data. The main effort of [12] is a procedure to adapt the prespecified LS steps of existing primary frequency control characteristics in order to gain an optimal LS plan by minimizing the total amount of shed load. Reference [11] proposes calculation of shed load at each stage of frequency relay in a stand-alone micro grid based on historical meteorological data and the Markov two-state model. Furthermore, the shed load is minimized and the lowest swing frequency is maximized using the Genetic Algorithm (GA). The work reported in [10] focuses on finding proper LS locations based on Voltage Stability Risk Index (VSRI) criteria which is calculated for each load bus using their voltage information that is assumed to be available through a synchrophasor based wide area monitoring and control system (WAMCS). The authors in [13] suggest the GA to minimize the shed load at each stage of under frequency relay. The predictive UFLS using frequency second derivative is proposed in [14] to forecast the frequency trajectory and overcome lack of data or wrong estimation of SFR method parameters.

According to [1], [9], and [10], the voltage deviation of load buses may be a proper and effective criterion of proximity to the event location. In order to find the most appropriate locations for LS plan, the frequency threshold of LS relays are almost instantly determined based on the voltage drop magnitude at their load bus. The present work benefits from locally measured frequency and voltage informations and hence implementation of proposed method is more affordable and simpler than the centralized LS methods which require fast and reliable communication systems [1].

This paper is organized as follows: The importance of voltage dynamics in analysis of the power system stability is investigated in Section II. The proposed solution to coordinate the UFLS and UVLS schemes under a new LS procedure is presented in Section III. The simulation set up and results are discussed in Sections IV and V, respectively. Finally, the paper is concluded in Section VI.

Manuscript received March 29, 2014; revised June 24, 2014, August 12, 2014, and August 17, 2014; accepted August 17, 2014. Paper no. TPWRS-00430-2014.

The authors are with the Department of Energy Technology, Aalborg University, Aalborg 9220, Denmark (e-mail: bho@et.aau.dk; b.hoseinzadeh@gmail.com; ffs@et.aau.dk; filipemfaria@hotmail.com; clb@et.aau.dk).

Digital Object Identifier 10.1109/TPWRS.2014.2351015

II. Necessity of Considering Voltage Dynamics in Power System Stability

Nowadays, the growing concern about the incidents initiated by voltage root causes has located in the center of attention [15]. Besides, assigning a separate category of instability classification to the voltage instability shows the importance of voltage dynamical behavior in the power system stability area [16]. The significance of voltage profile was stressed from different aspect of views in many literatures which are briefly reviewed in this section [5], [12].

The shortage of active power is often accompanied by deficit in reactive power and the lack of active/reactive power is reflected in the voltage profile of the load buses [9]. Any LS scheme in which the dependency of the loads to the voltage variation is overlooked may not be effective in practice.

According to [16], the voltage instability is a phenomena of a local nature and if it is not prevented in time by proper control actions, it may spread to neighbor areas and even to the entire power system. Since the frequency which is measured locally at load buses is a common factor across the whole network and does not contain useful information about the event location, the voltage instability and its geographical region may be detected only based on the voltage data.

In the decentralized control strategy which is the main effort of the present work, there is no communication link between relays involved with LS scheme. Therefore, the magnitude and location of the event are unavailable. Although, the aforementioned information are unknown and inaccessible in a decentralized LS scheme, the voltage deviation is linearly determined by them [17]. Hence, a more accurate and reliable measure of sensitivity to the scale and place of perturbation is the voltage deviation of load buses, i.e., a quantity that is locally available. The sensitivity of each individual load bus to a given incident may be reflected via their voltage deviation. It means that the load buses with more sensitivity to the disturbance, experience a larger voltage drop. Therefore, the load buses may be classified in term of their voltage drop which is proportional to their sensitivity.

Utilizing the voltage drop data in the centralized strategy of the LS program have been proposed by numerous literatures as an appropriate and efficient criterion for determining the location of disturbance [1], [7], [9], [10], but application of voltage decay has rarely been employed in the decentralized strategy, especially for online and dynamically determining the frequency thresholds of the LS relays.

III. Decentralized and Adaptive UFVLS Approach

A. Adaptive Tunning of Frequency Thresholds Using Voltage Drop Information

This paper addresses the decentralized strategy of the LS procedure and it assumes that there is no communication link between LS relays. Therefore, the only variables involved in the proposed method are the local voltage and frequency. In the traditional LS relays, the instantaneous value of voltage (for frequency measurement) and the rms value of voltage (for under voltage blocking function) are measured. Hence all of necessary informations required to implement in the proposed method are already accessible in a typical relay. As a result, there is no need to add extra hardware to the existing LS relays and modification of their algorithm (software programming) may be enough to realize the suggested approach [18].

The global chronological order of the load curtailment for the loads contributing in the LS scheme throughout the entire power system is arranged based on instantaneous voltage deviation from the pre-disturbance value. It means that, it is no longer necessary to set the frequency thresholds of the relays one by one manually in an off line procedure. A dynamic frequency threshold is automatically calculated and attributed to the relay stages instead of a constant, static and predefined frequency thresholds for the widespread range of disturbances. The frequency thresholds of different relays are continuously updated based on the voltage drop at the load buses. The buses with higher voltage decline are relatively allocated frequency thresholds closer to the upper limit of the permissible range (f_H). During the frequency decline, the frequency reaches these thresholds sooner and hence, the corresponding load feeders are shed earlier than the other load feeders. Depending on the magnitude of the voltage decay at the load buses, the frequency thresholds of distinct relays may have large differences, small differences, some overlap or even exactly same values.

In order to formulate the scheme mathematically, a frequency relay with m stages is considered in a given load bus which is participating in the LS scheme. The idea is formulated as follows:

$$\Delta v = v_{ss} - v \tag{1}$$

$$f_b^{th} = f_H - \Delta f_b^{th} \tag{2}$$

$$\Delta f_b^{th} = (f_H - f_L) \cdot \frac{(\Delta v_{\max} - \Delta v)}{\Delta v_{\max}} \tag{3}$$

$$f_i^{th} = f_b^{th} - (i-1) \cdot \Delta f_l^{th} \quad \forall i \in \mathbb{N}, 1 \le i \le m \tag{4}$$

$$\Delta f_l^{th} = (f_n - f_H) \cdot \frac{\Delta v}{\Delta v_{\max}} \tag{5}$$

where

- v is the voltage of the load bus;
- v_{ss} is the steady state value of voltage before the event/s;
- Δv is the voltage deviation from v_{ss};
- f_b^{th} is the base frequency threshold;
- f_H is the trigger frequency of the LS scheme;
- f_L is the lower limit of permissible frequency range;
- Δf_b^{th} is the base frequency threshold offset;
- $\Delta v_{\max}$ is the maximum voltage drop;
- f_i^{th} is the frequency threshold of the ith stage;
- i is the index of the stage;
- Δf_l^{th} is the local frequency threshold offset;
- m is the total number of stages;
- f_n is the nominal frequency of power system.

The voltage deviation of the load bus from the pre-disturbance value (v_{ss}) is calculated in (1). As reported in [19], the voltage profile may often have some natural minor fluctuations before and after the disturbance/s and even in the steady state condition. Since this type of inherent oscillations in real power systems may not be simulated properly by simulation software, therefore in order the scheme to be efficient in practice, the aforementioned fluctuations should be suppressed by an appropriate low pass filter to pass the significant voltage deviations only.

Each relay has a base frequency threshold (f_b^{th}) which specifies the relative position of frequency threshold deployment of the relay in the permissible frequency range and it is calculated

according to (2) using base frequency threshold offset (Δf_b^{th}). The base frequency threshold offset (Δf_b^{th}) in (3) indicates the proximity of the base frequency threshold (f_b^{th}) of the current relay to the trigger frequency of the LS scheme (f_H), which varies depending on the voltage drop of the load bus (Δv).

The frequency thresholds of different stages are calculated using base frequency threshold (f_b^{th}) and local frequency threshold offset (Δf_l^{th}) in (4). According to (4), the successive stages of the relay have a same local frequency threshold offset (Δf_l^{th}) which is also specified in (5) in term of voltage decay of the load bus (Δv).

In case of need to prioritize some special feeders of the load bus, this may be done in the proposed scheme by connecting the outputs of the relay with lower frequency thresholds (the stages with higher index of i) to the higher priority feeders [5]. It means that they will be among the last feeders to be shed in the aforementioned load bus.

Assigning a lower frequency threshold to a given feeder explicitly means that the feeder is relatively shed with some more delay rather than before, since it takes more time for the frequency to cross this lower frequency threshold. Thus, manipulating the frequency threshold of a given stage, indirectly changes the stage delay. This shows that there is a strong correlation between key parameters of the frequency relays such as frequency threshold and the delay between different stages and they are not completely independent.

B. Time Delay Between Consecutive Stages

The time delay between consecutive stages of the LS relay is another important key factor influencing the efficiency of the LS. The delays should be determined carefully to avoid unnecessary postpone in the load discarding process which may cause not only delayed control of frequency collapse instead of minimum possible time, but also may even allow the frequency to exit from permissible frequency range of the LS scheme (f_L to f_H) [20]. The delays need to be minimized to quickly restore the frequency to the acceptable continuous operating range as soon as possible [5], [11]. If the frequency collapse is not prevented by proper control actions in time, the generating units may be forced to operate out of their permissible boundary of frequency (± 0.5 Hz of their nominal range) for a period longer than the sustainable time of their frequency protection relay [5]. Therefore, the generating unit may be disconnected from the grid by the respective protection unit and the power system will encounter a much worse case called cascading events which may be harder than before to overcome due to the unpredictable dynamical behaviors of the power system.

Contrariwise, some literatures emphasize that too short delay time between successive stages may be unable to ignore any transient dips in the frequency profile [5], [21]. Besides, since the time gap between the moment that frequency reaches a given threshold and the moment in which the load is exactly shed typically requires 10 to 14 cycles of delay (relay and circuit breaker operating times) which needs to be considered as the minimum amount of delay in the algorithm [5]. Although, the stage time delays are not directly determined by the proposed scheme, they may vary from a few cycles to several seconds depending on the ROCOF and local frequency threshold offset (Δf_l^{th}) [5]. In order to respect the practical delays related to the relay and

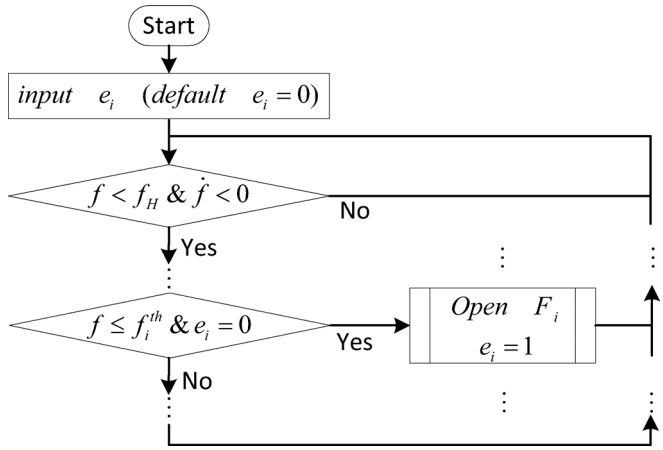

Fig. 1. Flowchart of the proposed LS scheme.

circuit breaker operating times, the minimum time between different stages of a given relay is determined as follows:

$$\Delta t \geq N \cdot T = \frac{N}{f_n} \tag{6}$$

where T and f_n are the time cycle of the sinusoidal waveform and nominal frequency of power system, respectively, and N is the number of delay cycles (N). The time between consecutive stages (Δt) may be estimated based on measured ROCOF from the relay bus bar and the local frequency threshold offset (Δf_l^{th}) calculated in (5) as follows [5]:

$$\dot{f} \cong \frac{\Delta f_l^{th}}{\Delta t}. \tag{7}$$

By extracting the term Δt from (7) and substituting in (6), the lower limit of Δf_l^{th} is approximated:

$$\Delta f_l^{th} \geq N \cdot \frac{\dot{f}}{f_n}. \tag{8}$$

The quantity of Δf_l^{th} calculated in (5) should also satisfy the inequality expressed in (8) as follows:

$$\Delta f_l^{th} = \max\left\{(f_n - f_H) \cdot \frac{\Delta v}{\Delta v_{\max}}, N \cdot \frac{\dot{f}}{f_n}\right\}. \tag{9}$$

C. Trigger Criterion of the LS Plan

The decision making process of the proposed LS scheme is illustrated in details as a flowchart in Fig. 1. Under normal condition, all of feeders (F_i) are connected to the load bus and their status bits are reset ($e_i = 0$), indicating that none of the stages have been operated yet. Several conditions need to be met in order to trigger the LS plan. The first condition is that the ROCOF quantity must be negative ($\dot{f} < 0$) as can be observed in the flowchart in Fig. 1. Although, this inequality needs to be satisfied, it may not be sufficient to trigger the LS scheme, since the ROCOF may have negative values due to the frequency fluctuations inside the permissible range. According to [5], instantaneous value of ROCOF may sometimes be misleading and the supervision of ROCOF value by another variable such as frequency may lead to a more secure LS scheme. The LS plan is triggered if the frequency declines below the trigger frequency of LS scheme (f_H) introduced in Section III-A. Besides, the

quantity of f_H should be carefully determined in order to provide sufficient response time for eventually available primary load/frequency controls or other countermeasures in the system [5], [22], as the LS plan is the last firewall and at the same time the most expensive solution against frequency collapse [12], [21].

The remaining checkpoints are associated with the distinct stages of the relay at different thresholds (f_i^{th}) which have been calculated in Section III-A. According to the rest of checkpoints in the flowchart, each individual feeder is disconnected if frequency profile crosses the frequency threshold of corresponding feeder and its status bit of the stage is zero ($e_i = 0$).

The number of assigned thresholds are selected based on the number of available stages in the employed relay (m) [12]. The higher frequency thresholds [corresponding to the lower values of i in (4)] are generally allocated to the feeders with lower priority by default, unless the arrangement has been manually changed by utility operators for any special reasons. As different arrangements of feeder priority may be chosen during the equipment installation, all of checkpoints are regularly checked in all iterations as can be seen in the flowchart. However, under any circumstances, the lower thresholds should be assigned to the feeders with higher priority. In case of having any uninterruptible loads, their status bit may be manually set ($e_i = 1$) using either provided hardware switches or user interface panel available on the protection device in order to avoid their outage under any conditions. The new settings are applied to the LS procedure when the next restart of the microprocessor relay takes place at the initialization phase of registers.

IV. Simulation Setup

In order to evaluate the effectiveness of the proposed control scheme, the 39 bus IEEE standard test system depicted in Fig. 2 is selected as case study [6], [10], [23]. The 4th-order SM model is used for all generators. The SMs are equipped with the IEEE standard governor GOV-IEESGO and automatic voltage regulator AVR-IEEEX1. The details of the system data can be accessed in [23].

The dependency of load's active and reactive power to the voltage and frequency in term of different type of loads is defined in (10) and (11) [5]. Moreover, the relevant parameters and the Share (s) of different types of loads such as type i, c and p in the load model is given in Table I of [16, Appendix]:

$$P = P_0 \cdot \left[s_i \cdot \left(\frac{v}{v_0}\right)^{e_i^{pv}} + s_c \cdot \left(\frac{v}{v_0}\right)^{e_c^{pv}} + s_p \cdot \left(\frac{v}{v_0}\right)^{e_p^{pv}} \right] \cdot \left[s_i \cdot \left(\frac{f}{f_0}\right)^{e_i^{pf}} + s_c \cdot \left(\frac{f}{f_0}\right)^{e_c^{pf}} + s_p \cdot \left(\frac{f}{f_0}\right)^{e_p^{pf}} \right] \quad (10)$$

$$Q = Q_0 \cdot \left[s_i \cdot \left(\frac{v}{v_0}\right)^{e_i^{qv}} + s_c \cdot \left(\frac{v}{v_0}\right)^{e_c^{qv}} + s_p \cdot \left(\frac{v}{v_0}\right)^{e_p^{qv}} \right] \cdot \left[s_i \cdot \left(\frac{f}{f_0}\right)^{e_i^{qf}} + s_c \cdot \left(\frac{f}{f_0}\right)^{e_c^{qf}} + s_p \cdot \left(\frac{f}{f_0}\right)^{e_p^{qf}} \right]. \quad (11)$$

Since in practice, shedding the feeders of the load buses are possible instead of shedding a specific amount of load, the proposed scheme deals with selection of proper feeders in order the approach to be implemented in practice. The loading percentage of distinct feeders in term of different loads of the test system is presented in Table II of Appendix. For the sake of comparing the result of proposed scheme (AUFVLS) to the conventional UFLS, the parameters of both methods are available in Table III [2] of the Appendix.

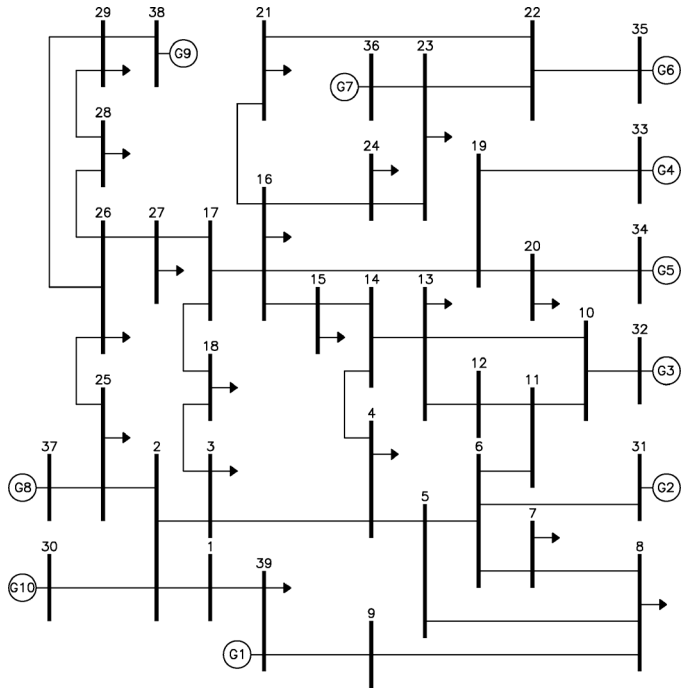

Fig. 2. The 39-bus IEEE standard test system.

V. Simulation Results and Discussion

In order to assess the efficiency of the proposed scheme, a set of numerical simulations is conducted in DIgSILENT PowerFactory 15.0 software. Three different scenarios with severe contingencies in distinct areas of the power system, e.g., multiple cascading events, small and big islanding with various active/reactive power deficit level have been chosen as disturbance and the results are compared to the performance of the conventional UFLS scheme. The goal is to return the frequency and bus voltages back to the permissible range in acceptable time period and localizing the LS plan as much as possible close to the event location.

A. Scenario 1

In the first scenario, cascading events including outage of generator G9 connected to the bus 38 at 2 s as the initiating event followed by overloading and hence tripping the transmission line 16–19 at 5 s (Fig. 2) is considered as a serious disturbance with the capacity of 1970 MW ($\sim 32\%$ of system generation). Figs. 3–6 show the simulation results throughout 60 s of time simulation. The power system is in the steady state before the first event at 2 s and all of variables are in the normal range such as frequency which is stable at f_n.

The line outage creates a small island including buses 19, 20, 33, and 34, generators G4 and G5, and the load 20 beside of the rest of the power system. The frequency of island starts to increase up to 62.5 Hz as a result of exceeding the generation from the existing load. Bringing the frequency of the island (Fig. 3) down to the normal range is basically fulfilled by reducing the

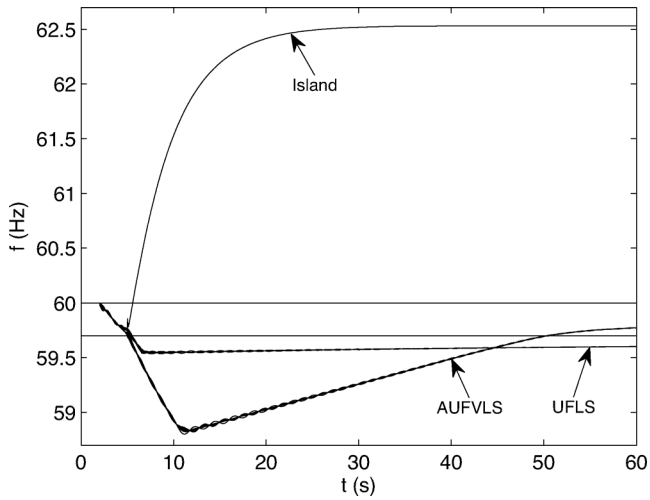

Fig. 3. Scenario 1: the grid and island frequencies.

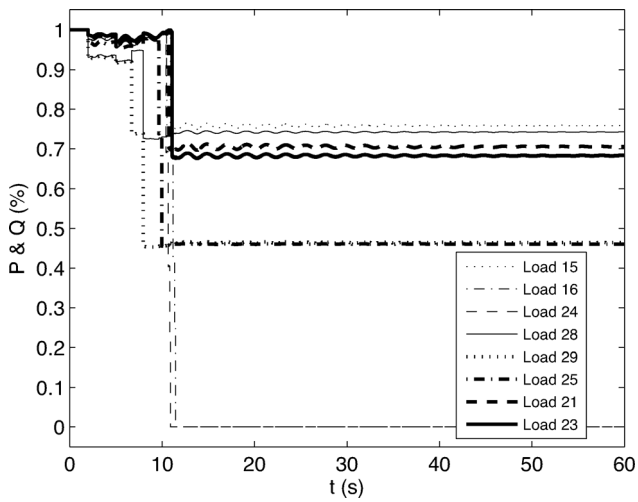

Fig. 4. Scenario 1: the chronological order of LS (AUFVLS).

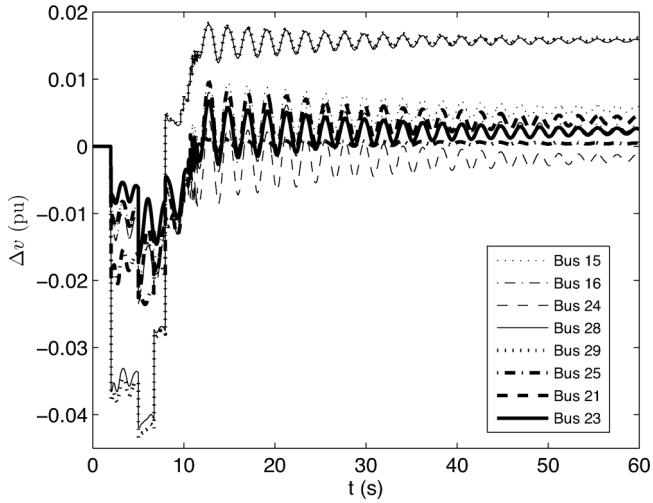

Fig. 5. Scenario 1: the voltage deviation from v_{ss} (AUFVLS).

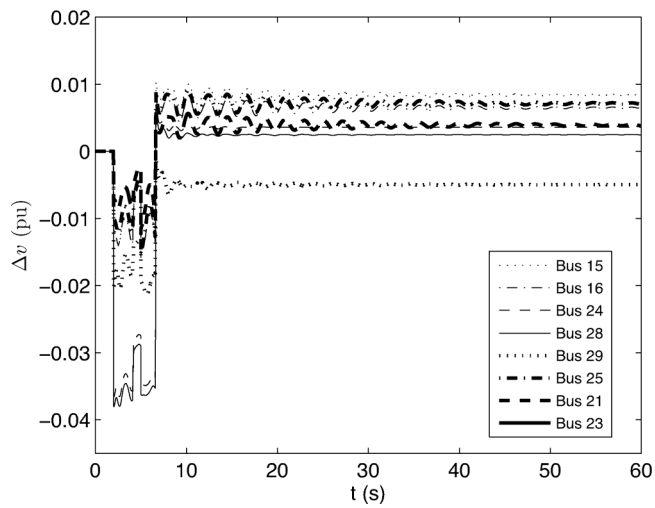

Fig. 6. Scenario 1: the voltage deviation from v_{ss} (UFLS).

generation through relevant primary and maybe secondary control and therefore is out of scope of the LS scheme duty.

Although the voltage profile of both proposed method (AUFVLS) and conventional UFLS scheme are in the range and the UFLS yields better post-disturbance steady state voltage values, the UFLS is unable to bring the frequency back to the acceptable range above f_H. There is the risk of more cascading events (outage of other SMs) in case of no or insufficient spinning reserve and maintaining the frequency below the trigger frequency of underfrequency protection relay of the SMs beyond their tolerated time [5].

Moreover, the UFLS method involves all of nearby and distant power system loads (19 loads) except the load 20 which is located inside the island. Involving all of system loads in the LS program is unpractical and is not recommended at all [6]. Distributing the active power deficit between all 19 loads of the network results less dispersion in bus voltage values as mentioned before, whereas the AUFVLS method deals with only 8 loads in the vicinity of the perturbation place which have been mentioned in the legend of Figs. 4 and 6. The chronological order of the load curtailments demonstrated in Fig. 4 in which the loads 16 and 24 are completely shed and the loads 25, 29, 21, 28, 23, and 15 are partially curtailed.

B. Scenario 2

The second scenario consists of 4 cascading events in which the transmission lines 16–17, 25–26, 2–3, and 3–4 are tripped consecutively due to their overloading condition at 2, 4, 5, and 6 s, respectively (Fig. 2). As a result, a big island including G9 and loads 29, 28, 26, 27, 18, and 3 is separated from the rest of the power system with G9 as the new reference machine (slack bus) in the island. The load-generation mismatch in the island is about 564 MW ($\sim 68\%$ of remained generation) which may be accounted as a very severe contingency. Figs. 7–10 show the simulation results of scenario 2 throughout 60 s of time simulation.

Unlike the previous scenario in which the island suffers from over generation, in this case the rest of power system experiences the surplus generation (Fig. 7) and the frequency of grid is stabilized at almost equal to 61 Hz. Although in the incipient phase of LS process, the UFLS method prevents the frequency downfall in a higher value and even sooner than AUFVLS, the

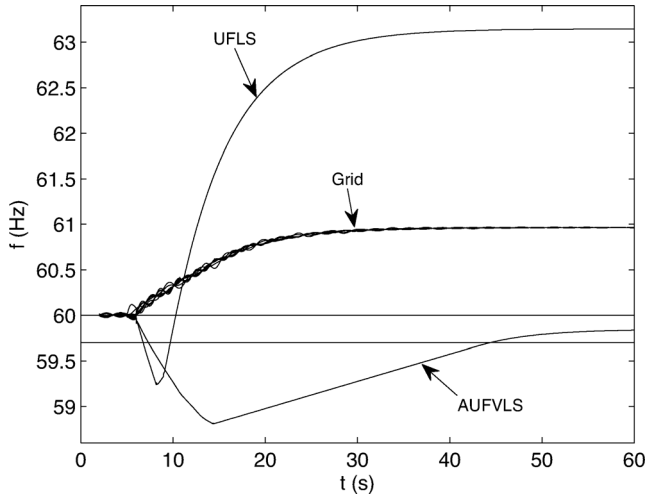

Fig. 7. Scenario 2: the island and grid frequencies.

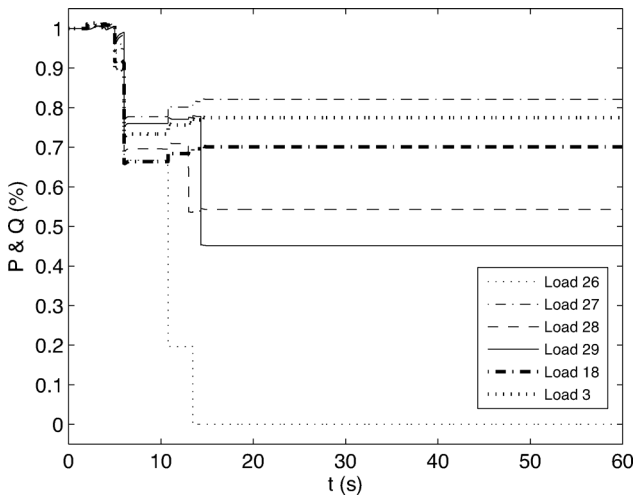

Fig. 8. Scenario 2: the chronological order of LS (AUFVLS).

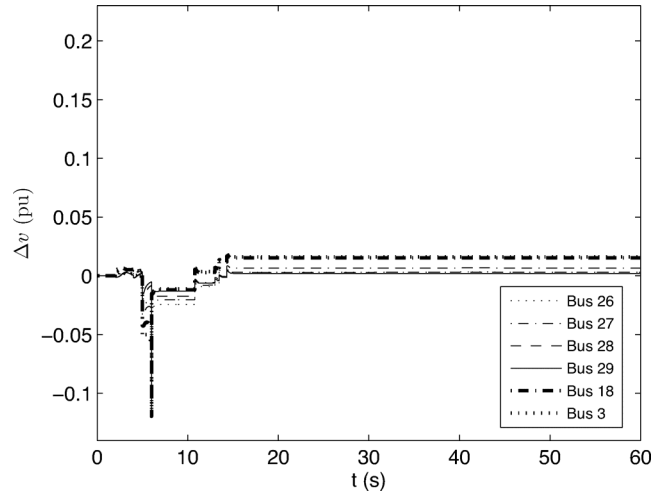

Fig. 9. Scenario 2: the voltage deviation from v_{ss} (AUFVLS).

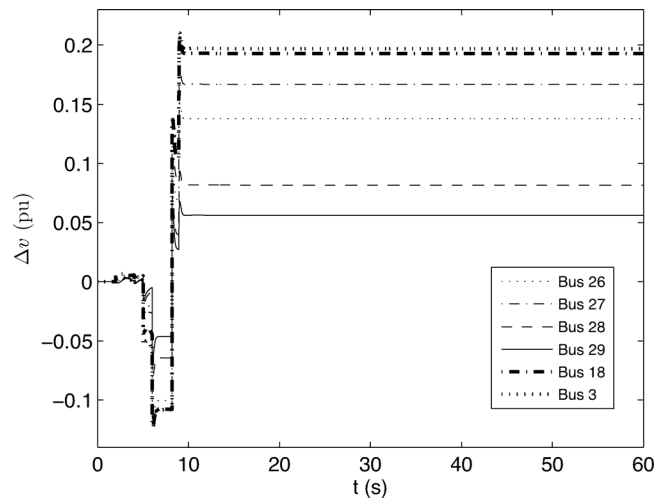

Fig. 10. Scenario 2: the voltage deviation from v_{ss} (UFLS).

UFLS is inefficient in post-disturbance steady state value of frequency beyond 63 Hz and the island suffers from over LS which is undesired. In contrast, the AUFVLS stabilizes the frequency inside the acceptable boundary with remarkably less voltage deviations in the load buses. By comparing the voltage profile of both AUFVLS and UFLS methods presented in Figs. 9 and 10, respectively, it is demonstrated that the proper LS decisions may not be always made by UFLS method, i.e., shedding the loads with higher voltage decay. The incorrect distribution of load curtailment in UFLS method leads to voltage profiles out of range ($\Delta v_{\max}$) which may damage the equipments of both utility and customers.

On the contrary to the previous scenario in which the target area of the LS scheme was almost the whole of the network, in current scenario the target area is a small part of the network and therefore the selection set of loads participating in the LS plan are same for both methods (loads 26, 27, 28, 29, 18, and 3). It means all of loads are almost close to the event locations (tripped lines) and are influenced by the perturbation.

The differences between the methods are due to the differences in the selection set of feeders rather than the loads. In the UFLS method, all of distant and nearby loads are contributing in the LS plan with the same number of feeders due to the same frequency thresholds which have already been predefined off line for the same stages. Inversely, the AUFVLS method triggers different number of feeders for each individual load, depending on their bus voltage deviation. In this case, 4 stages of load 26, 2 stages of loads 29 and 28, and one stage of loads 27, 18, and 3 are totally rejected (Fig. 10).

C. Scenario 3

The cascading events of the current scenario occur in a place far from two previous scenarios. The transmission line 6–11 is suddenly lost at 2 s followed by over loading of line 4–14 which results outage of it at 4 s. The two remaining power flow paths to this area (lines 1–39 and 3–4) are overloaded in a same manner and are simultaneously disconnected at 5 s. Finally, the area consisting of generator G1 and the loads 39, 4, 7, and 8 is islanded at 5 s. A relatively large island is separated from the rest of the power system with generator G1 as the reference machine (slack bus). The load-generation mismatch in the island is about 1347 MW ($\sim 135\%$ of remained generation) which may be considered as a challenging contingency.

Figs. 11–14 demonstrate the simulation results of this scenario. According to the Fig. 11, same as the previous scenario, the reaction of the UFLS method to the event is faster in comparison to the performance of AUFVLS, but from steady state

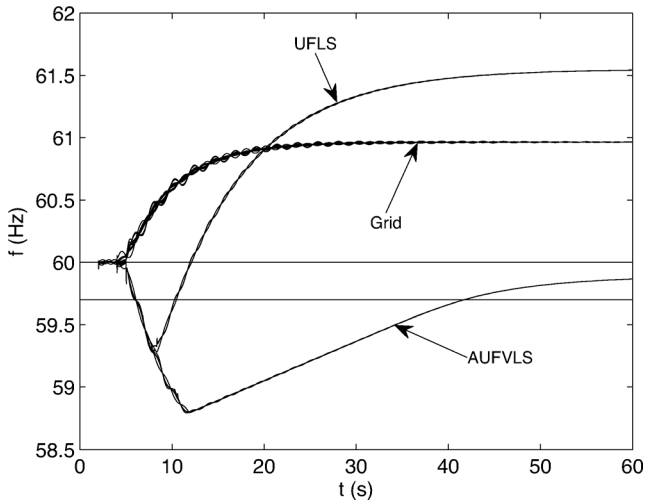

Fig. 11. Scenario 3: the island and grid frequencies.

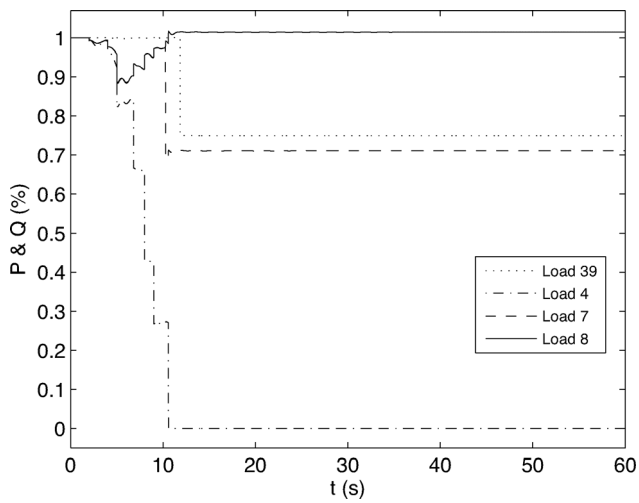

Fig. 12. Scenario 3: the chronological order of LS (AUFVLS).

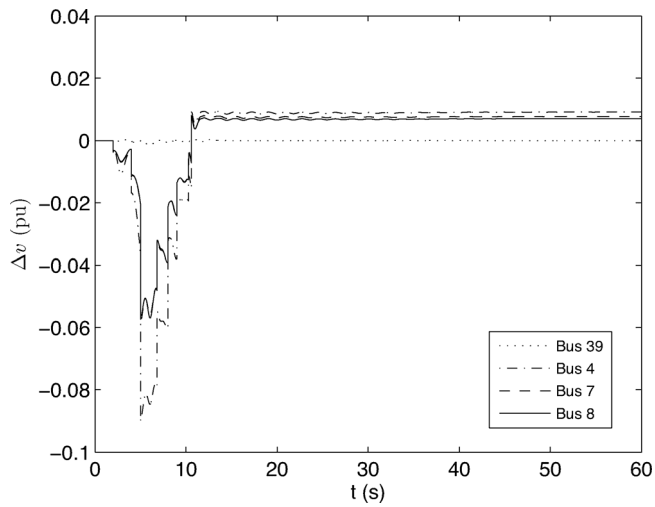

Fig. 13. Scenario 3: the voltage deviation from v_{ss} (AUFVLS).

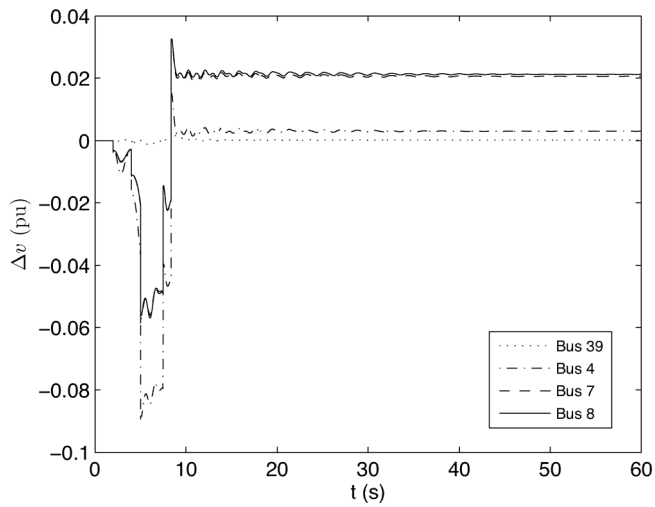

Fig. 14. Scenario 3: the voltage deviation from v_{ss} (UFLS).

frequency aspect of view, the response of UFLS method (frequency above 61.5 Hz) is not acceptable due to the unnecessary extra LS, while the frequency is settled in time inside the permissible range by AUFVLS method.

Comparing the voltage profiles of both UFLS and AUFVLS methods (Figs. 13 and 14) reveals that the performance of AUFVLS in the post-disturbance load bus voltages, i.e., having voltages closer to the pre-disturbance values, are much better than UFLS method. In the AUFVLS method 4, 1, and 1 stages of the loads 4, 39 ,and 7 are shed, respectively (Fig. 12), whereas in the UFLS method the first two stages of all of available loads (4, 7, 8, and 39) in the island are curtailed. In order to compare AUFVLS with UFLS method from shed load aspect of view, the total shed load in term of methods and scenarios is shown in Table IV of the Appendix. Due to the insufficient LS in scenario 1, the UFLS method is unable to return the frequency to the permissible range (Fig. 3) and in the scenarios 2 and 3, the UFLS method causes over LS (Figs. 7 and 11) which are not desired.

By comparing the frequency profile of different scenarios, it can be revealed that AUFVLS causes more smooth frequency behavior (advantage) due to provision of different frequency thresholds which are determined based on voltage drop at load buses and hence avoiding large *shocks* resulting from simultaneous shedding of corresponding stages in distinct loads due to the same frequency threshold as happens in classical UFLS.

VI. Conclusion

The loads closer to the event location experience a larger voltage drop and need to be shed first. In this paper the frequency thresholds of the LS relays are determined on line based on their voltage deviation from the pre-disturbance value. The frequency thresholds are adaptively specified based on location and magnitude of the disturbance/s. It means that higher frequency thresholds are assigned to the LS relay of the loads that experience more voltage decay. Different scenarios of severe contingencies including cascading, combinational events and islanding confirm that the setting of protection equipments may be dynamically, rapidly and properly determined according to the current status of the power system.

Appendix

Table I lists the voltage and frequency dependency of loads; Table II lists the load percentage of feeders before the disturbance/s; Table III lists the simulation parameters of different methods; and Table IV lists the total shed load (MW).

TABLE I
VOLTAGE AND FREQUENCY DEPENDENCY OF LOADS

Load type	Share (s)(%)	pv	pf	qv	qf
Light bulb (i)	10	1.6	0.0	0.0	0.1
Fluorescent bulb (c)	20	1.2	-1.0	3.0	-2.8
Asynchronous motor (p)	70	0.1	2.8	0.6	1.8

TABLE II
LOAD PERCENTAGE OF FEEDERS BEFORE THE DISTURBANCE/S

Load	F1	F2	F3	F4	Load	F1	F2	F3	F4
3	25	30	20	25	**23**	32	16	28	24
4	25	29	18	28	**24**	30	29	19	22
7	30	29	19	22	**25**	25	29	18	28
8	18	30	23	29	**26**	30	23	27	20
12	28	18	30	24	**27**	19	29	18	34
15	25	29	18	28	**28**	28	18	30	24
16	25	32	17	26	**29**	22	33	25	20
18	32	18	23	27	**31**	19	29	18	34
20	18	30	23	29	**39**	25	28	27	20
21	30	23	27	20					

TABLE III
SIMULATION PARAMETERS OF DIFFERENT METHODS

Method	Parameters				
UFLS	f^{th} (Hz)	59.7	59.5	59.3	59.1
	T_d (cycle)	60	30	18	6
AUFVLS	f_n=60 Hz, f_L=57.9 Hz, f_H=59.7 Hz, m=4, N=12 and Δv_{max}=0.2 pu				

TABLE IV
TOTAL SHED LOAD (MW)

Method	Scenario 1	Scenario 2	Scenario 3
UFLS	1159	1036	1243
AUFVLS	1213	934	570

REFERENCES

[1] A. Saffarian and M. Sanaye-Pasand, "Enhancement of power system stability using adaptive combinational load shedding methods," *IEEE Trans. Power Syst.*, vol. 26, no. 3, pp. 1010–1020, Aug. 2011.

[2] V. V. Terzija, "Adaptive underfrequency load shedding based on the magnitude of the disturbance estimation," *IEEE Trans. Power Syst.*, vol. 21, no. 3, pp. 1260–1266, Aug. 2006.

[3] Y.-Y. Hong and S.-F. Wei, "Multiobjective underfrequency load shedding in an autonomous system using hierarchical genetic algorithms," *IEEE Trans. Power Del.*, vol. 25, no. 3, pp. 1355–1362, Jul. 2010.

[4] D. Prasetijo, W. Lachs, and D. Sutanto, "A new load shedding scheme for limiting underfrequency," *IEEE Trans. Power Syst.*, vol. 9, no. 3, pp. 1371–1378, Aug. 1994.

[5] *IEEE Guide for the Application of Protective Relays used for Abnormal Frequency Load Shedding and Restoration*, IEEE Std. C37.117-2007, 2007.

[6] J. Tang, J. Liu, F. Ponci, and A. Monti, "Adaptive load shedding based on combined frequency and voltage stability assessment using synchrophasor measurements," *IEEE Trans. Power Syst.*, vol. 28, no. 2, pp. 2035–2047, May 2013.

[7] M. Q. Ahsan, A. H. Chowdhury, S. S. Ahmed, I. H. Bhuyan, M. A. Haque, and H. Rahman, "Technique to develop auto load shedding and islanding scheme to prevent power system blackout," *IEEE Trans. Power Syst.*, vol. 27, no. 1, pp. 198–205, Feb. 2012.

[8] P. Kundur *et al.*, "Definition and classification of power system stability IEEE/CIGRE joint task force on stability terms and definitions," *IEEE Trans. Power Syst.*, vol. 19, no. 3, pp. 1387–1401, Aug. 2004.

[9] U. Rudez and R. Mihalic, "Analysis of underfrequency load shedding using a frequency gradient," *IEEE Trans. Power Del.*, vol. 26, no. 2, pp. 565–575, Apr. 2011.

[10] K. Seethalekshmi, S. Singh, and S. Srivastava, "A synchrophasor assisted frequency and voltage stability based load shedding scheme for self-healing of power system," *IEEE Trans. Smart Grid*, vol. 2, no. 2, pp. 221–230, 2011.

[11] Y.-Y. Hong, M.-C. Hsiao, Y.-R. Chang, Y.-D. Lee, and H.-C. Huang, "Multiscenario underfrequency load shedding in a microgrid consisting of intermittent renewables," *IEEE Trans. Power Del.*, vol. 28, no. 3, pp. 1610–1617, Jul. 2013.

[12] U. Rudez and R. Mihalic, "Monitoring the first frequency derivative to improve adaptive underfrequency load-shedding schemes," *IEEE Trans. Power Syst.*, vol. 26, no. 2, pp. 839–846, May 2011.

[13] Y.-Y. Hong and P.-H. Chen, "Genetic-based underfrequency load shedding in a stand-alone power system considering fuzzy loads," *IEEE Trans. Power Del.*, vol. 27, no. 1, pp. 87–95, Jan. 2012.

[14] U. Rudez and R. Mihalic, "A novel approach to underfrequency load shedding," *Elect. Power Syst. Res.*, vol. 81, no. 2, pp. 636–643, 2011.

[15] Y. Wang, I. Pordanjani, W. Li, W. Xu, and E. Vaahedi, "Strategy to minimise the load shedding amount for voltage collapse prevention," *IET Gener., Transm., Distrib.*, vol. 5, no. 3, pp. 307–313, 2011.

[16] P. Kundur, *Power System Stability and Control*. Noida, India: Tata McGraw-Hill Education, 1994.

[17] H. Liu, A. Bose, and V. Venkatasubramanian, "A fast voltage security assessment method using adaptive bounding," *IEEE Trans. Power Syst.*, vol. 15, no. 3, pp. 1137–1141, Aug. 2000.

[18] A. Ghaleh, M. Sanaye-Pasand, and A. Saffarian, "Power system stability enhancement using a new combinational load-shedding algorithm," *IET Gener., Transm., Distrib.*, vol. 5, no. 5, pp. 551–560, 2011.

[19] D. Karlsson and D. J. Hill, "Modelling and identification of nonlinear dynamic loads in power systems," *IEEE Trans. Power Syst.*, vol. 9, no. 1, pp. 157–166, Feb. 1994.

[20] H. Bevrani and A. Tikdari, "An ANN-based power system emergency control scheme in the presence of high wind power penetration," in *Wind Power Systems*. New York, NY, USA: Springer, 2010, pp. 215–254.

[21] B. Hoseinzadeh, F. F. D. Silva, and C. L. Bak, "Power system stability using decentralized under frequency and voltage load shedding," in *Proc. IEEE PES General Meeting 2014*, 2014.

[22] B. Hoseinzadeh and Z. Chen, "Intelligent load-frequency control contribution of wind turbine in power system stability," in *Proc. 2013 IEEE EUROCON*, 2013, pp. 1124–1128.

[23] H. Bevrani, F. Daneshfar, and R. Daneshmand, "Intelligent power system frequency regulations concerning the integration of wind power units," in *Wind Power Systems*. New York, NY, USA: Springer, 2010, pp. 407–437.

Bakhtyar Hoseinzadeh (S'13) received the B.Eng. and M.Eng. degrees from Sahand University of Technology, Tabriz, Iran, in 1999 and Iran University of Science & Technology, Tehran, Iran, in 2001, respectively. He is currently pursuing the Ph.D. degree in the Department of Energy Technology, Aalborg University, Denmark.

From 2001 to 2012, he was with University of Kurdistan as Research Assistant. His research interests include renewable energy sources (RESs) and power system stability.

Filipe Miguel Faria da Silva (M'09) was born in Portugal in 1985. He received the M.Sc. degree in electrical and computers engineer from Instituto Superior Tecnico, Portugal (IST-UTL), in 2008 and the Ph.D. degree from Aalborg University, Denmark, in 2011.

He is currently an Associate Professor in the Department of Energy Technology, Aalborg University, where he is also semester coordination of the Electrical Power System and High Voltage Engineering master program and vice-leader of the Modern Power Transmission Systems research program. His research focuses on power cables, electromagnetic transients, system modeling, HVDC transmission, and HV phenomena, having authored dozens of articles and a book in these areas. He is currently supervising projects in the areas of power cables, network stability, and high voltage phenomena.

Prof. Faria da Silva is a member of CIGRE.

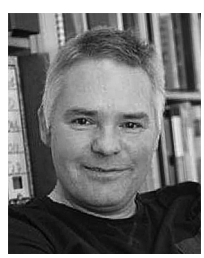

Claus Leth Bak (SM'99) was born in Rhus, Denmark, on April 13, 1965. He received the B.Sc. degree with honors in electrical power engineering in 1992 and the M.Sc. degree in electrical power engineering from the Department of Energy Technology (ET) at Aalborg University (AAU), Denmark, in 1994.

After his studies, he worked as a professional engineer with Electric Power Transmission and Substations with specializations within the area of Power System Protection at the NV Net Transmission Company. In 1999, he was employed as an Assistant Professor at ET-AAU, where he holds a Professor position today. He has supervised 15 Ph.D. students and more than 50 M.Sc. theses. His main research areas include Corona Phenomena on Overhead Lines, Power System Modeling and Transient Simulations, Underground Cable transmission, Power System Harmonics, Power System Protection, and HVDC-VSC Offshore Transmission Networks. He is the author/coauthor of approximately 120 publications.

Prof. Bak is a member of Cigr JWG C4-B4.38, Cigr SC C4 study committee member and Danish Cigr National Committee.